

Multilayer Micro Bio Chip for Intra Organelle Nanoporation

Prof (Dr) Swarup Sarkar

Department of Electronics and communication engineering,
SMIT, Sikkim Manipal University,
Sikkim, India

Email : swarupsarkar957@yahoo.com

Abstract:- Present research paper represents that the intra organelle nano poration of multi layer osteoblast cell placed in a 3D non uniform micro fluidic chip composed of bi metallic heterogeneous micro electrode under the influences of smart control FPGA based pico pulse generator and images of intra organelle nanoporation are recognized experimentally. It is observed that When the micro pulse is applied the cell starts to response but it is unable to penetrate the intra cellular nucleus- membrane where as the expected results will come when the Pico pulse is applied on the cell, a number of nano pores are generated on the intra organelle and chemicals are entered into the cell. It is also exposed that the key parameter of nanoporation such as intra pore density and ion uptake are externally controlled by user defined hybrid 3D micro chip and FPGA based pico pulse generator.

Keywords: Pico seconds Pulsed Electric Field (psPEF), Bi metallic electrode, intrigrated bio Micro chip, Dense Osteoblast cell, Intra-organelle, nanoporation

I INTRODUCTION

In recent developments of micro technologies and micro fluidics techniques permit consideration of the design and fabrication of new innovative tools for biology [1]. The main benefits of these technologies consist in their miniaturization and parallelization capabilities, as well as real-time observation in the case where transparent materials are used for the device fabrication. The use of micro fluidic devices in nanoporation is a remarkable exploration in the field of drug delivery system[2]. Although the nanoporation process itself in sophisticated devices with full control over the process as well as cell debris separation and subsequent intracellular cell content analysis have not been reported yet[3]. Therefore, it is expected that integrated devices where combinations of electroporation, separation and analysis occur will emerge, such as devices with integrated chromatography, electrophoresis or isoelectric focusing steps for separation, and mass spectroscopic, electrochemical and fluorescent methods for analysis[5]-[9]. Secondly, the present designs usually require multiple manual steps in order to insert the cells, electroporation them and measure the effects. Until now, no devices have been reported where all of these steps have been integrated in an automated way, preferably with multiple samples in 482 parallel, which could greatly enhance the application of micro technological analysis. Inspire of this the proper and efficient reorganization of cell nanoporative image is a new challenge for the scientists [10]-[14]. To consider all above limitations the author design a 3D non uniform micro fluidic chip composed of bi metallic heterogeneous micro electrode under the influences of smart control FPGA based pico pulse generator and study the intra organelle nanoporation of rigid cell like osteoblast. This biochip composed of bi metallic (Bi and Au) hybrid sidewall electrodes and multi dimensional micro fluidic channel that is described to deliver a maximum of energy to the medium containing multilayer osteoblast cell.

In this research paper we explore the design and fabrication of 3D hybrid micro bio chip along with its electric field strength analysis. We also address the mathematical modeling of osteoblast intraorganelle nanoporation and its characterization through optimum experiments and we also study effect of Pico electric field on intraorganelle nanoporation of osteoblast cell through this research article.

II. THEATRICAL ANALYSIS OF INTRA ORGANELLE NANOPORATION

A Theoretical analysis of different parameters of intraorganelle nanoporation

(i). Intra organelle voltages

C.Yao gave the following Schematic diagram of double -shelled spherical cell in suspension, which is used for theoretical explanation of outer and inner membrane potential of a biological cell[11],[15]-[19].

After simplification of equation we get the outer membrane potential ($V_{org(o)}(t)$) and inner membrane potential $V_{org(i)}(t)$ is as follows

$$V_{org(o)}(t) = 1.5 R_c E(t) \left[-e^{-\frac{t}{\tau_{cell}}} - 1(t - \tau) + e^{-\frac{t-\tau}{\tau_{cell}}} \cdot 1(t - \tau) \right] \cos \theta$$

$$V_{org(i)}(t) = \frac{1.5 \tau_{cell} R_{nuc} E(t)}{\tau_{cell} - \tau_{nuc}} \left[\left(e^{-\frac{t}{\tau_{cell}}} - e^{-\frac{t}{\tau_{nuc}}} \right) - \left(e^{-\frac{t-\tau}{\tau_{cell}}} - e^{-\frac{t-\tau}{\tau_{nuc}}} \right) \cdot 1(t - \tau) \right] \cos \theta$$

As we know that $E(t) = v/d$, where v =applied voltage & d =distances in between two electrode.

(ii) Calculation of the radius of nanopores:

Based on the theory of membrane permeabilization [13], nano pores are initially created with a radius of r^* . By increasing the applied electric field, nano pores start to develop in order to minimize the energy of the cell membrane. For the intra organelle with n nanopores, the rate of change of their radius of pore(r), can be determined by the following set of equations: [15]-[19]

$$U(r, Vn, Ap) = \frac{D}{KT} \left\{ 4\beta \left(\frac{r^*}{r} \right)^4 \frac{1}{r} - 2\pi\gamma + 2\pi\sigma r + \frac{[\Delta\varphi]^2 Fmax}{1 + rh/(r + ri)} \right\}$$

Where D is the diffusion co efficient, K = boltz man constant, T =absolute temp, $\varphi(r, \theta)$ =intra organelle potential. γ = surface tention. The constants of the above equations are defined in Table 1.

(iii) Calculation of the intra organelle pore current

On the other hand from the some references we have come to know that the outer & inner membrane pores current are expressed respectively [13]

$$I_{epi} = \frac{\pi r m^2 \sigma \Delta\varphi}{Fh} * \frac{e^{(\Delta\varphi - 1)}}{w_0 * e^{(w_0 - nvn(t))} - n\Delta\varphi} * \frac{e^{\Delta\varphi(t)} - X}{w_0 - nV(t)}$$

$$\text{And } X = \frac{w_0 * e^{(w_0 + nvn(t))} + n\Delta\varphi}{w_0 + nV(t)}$$

Where I_{epi} Intra organelle pore current.

(iv) Calculation of the intra organelle pressure

From various literature surveys[15]-[19], it is come to know that when electric field is applied on a biological cell specific pressure is inserted into the membrane which is mathematically expressed as

$$P_i = \frac{\epsilon n \Delta\varphi^2}{2h^2}$$

(v) Ccalculation of the intra organelle surface tension

As we know when the electric field is applied on the biological cell its molecular & chemical property are changes which may cause the change of surface tension which is mathematically expressed as

$$\Gamma_{in} = \frac{2 * \epsilon n * \Delta\varphi}{hi}$$

Where Γ_{in} is the surface tension of intra organelle and hi are the thickness of inner membrane.

(vi) Calculation of the intra organelle pore density

DeBruin KA, Krassowska W (1999a) exposed that the rate of creation of nanopores at intra organelle can be found as [15]-[19]

$$\frac{dN(t)}{dt} = \alpha * e^{(\Delta\varphi/V_{ep})^2} \left(1 - \frac{N(t)}{Neq(Vn)} \right)$$

Where $N(t)$ is the pore density.

(vii) Calculation of the intra organelle ion uptake:

It is known from the bio chemistry that the ion uptake can be calculated by following mathematical calculation [14] ,[15]-[19],

$$I_{uptake} = Kf \left[1 - \left(1 + Kp \cdot te \left(1 + \frac{Kp \cdot te}{2} \right) \right) * e^{-Kp \cdot te} \right]$$

Where $Kf = \frac{D \cdot Sc}{Vc \cdot d}$, and $Kp = e^x$,

$$x = \left[\frac{9 \cdot \Delta R \cdot Vp \cdot a^2 \cdot \epsilon_0 (\epsilon w - \epsilon c)}{8 \cdot Kb \cdot T \cdot d^2} \right] * Vn^2$$

D = Diffusion co efficient,

Vc = Area of the pore,

d = thickness. $Sc = N \cdot \pi \cdot r^2$,

$\Delta R \cdot Vp = \pi \cdot d (r_1^2 - r^2)$, $T = T_{emp}$ in kelvin.

Kb =Boltz man constant. ϵw =permittivity of water,

ϵc = permittivity of cytoplasm. te = pulse duration.

r_1 = radius of pore , r =radius of initial pores,

$V_{org(t)}$ =intra organelle potential.

III NUMERICAL SIMULATION

In this study, above Equations are solved numerically to find the each and every parameters of nanoporation to investigate the creation of nano-pores on the cell membrane. The Mat lab 7.2 & Comsol-4.3a, commercial package was used in the numerical simulations. In order to discrete the solution domain, unstructured meshes were applied. The solution domain was broken into small meshes to allow meshes to fully cover the solution domain without overlapping.

IV RESULT AND DISCUSSION

A Mathematical modeling of nanoporation

The electroporation process, including the formation and expansion of the pores, are described by the Smoluchowski partial differential equation. The Smoluchowski equation defines a pore density function, $n(r, t)$, such that the number of pores with radius between r and $r + dr$ at any given time, t , is $n(r, t)dr$. $n(r, t)$ is described as

$$\frac{\partial n}{\partial t} + D \frac{\partial}{\partial r} \left(- \frac{\partial n}{\partial r} - \frac{n}{kT} \frac{\partial W}{\partial r} \right) = S(r)$$

Where D is the pore diffusion coefficient, r is the pore radius, W is the formation energy of a pore with radius r , and $S(r)$ describes the transition of hydrophobic pores to hydrophilic ones, as

$$S(r) = \frac{v_c}{kT} h \frac{\partial W_0}{\partial r} e^{W_0/kT} - v_d nH(r_* - r)$$

where v_c is the pore creation rate, h is the membrane thickness, W_0 is the formation energy of a hydrophobic pore, v_d is the pore destruction rate, r_* is the radius at which

hydrophobic and hydrophilic pores have the same energy, and $H(r^*-r)$ is a step function at $r = r^*$. Assuming that, (i) the expansion of the pores is negligible, and (ii) the temporal change of the minimum pore energy is negligible, a quasistatic asymptotic model of electroporation simplifies the PDE equation to an ordinary differential equation. The ODE defines the pore density, $N(t)$, which is related to $n(r, t)$ as

$$N(t) = \int_{r=0}^{\infty} n(r, t) dr$$

The quasistatic asymptotic equation for $N(t)$ is

$$\frac{dN(t)}{dt} = \alpha e^{(V_m(t)/V_{ep})^2} \left(1 - \frac{N(t)}{N_0} e^{-q(V_m(t)/V_{ep})^2} \right)$$

Where V_m is the transmembrane voltage, V_{ep} is the characteristic voltage of electroporation, N_0 is the equilibrium pore density at $V_m = 0$, and a and q are constants.

It is reported that, when the transmembrane voltage achieves the required voltage of electroporation some pores are formed in the membrane. The formation of the pores increases the membrane conductivity of the membrane and is electrically modeled as an additional current density, J_{ep} , inside the membrane. J_{ep} is written as

$$J_{ep}(t) = N(t) \frac{\pi r_p^2}{h} \sigma_p V_m K$$

Where N is the density of the pores, r_p is the pore radius, σ_p is the conductivity of the solution inside the pore, V_m is the transmembrane voltage, h is the thickness of the Membrane, and K is

$$K = \frac{e^{v_m} - 1}{\frac{\omega_0 e^{\omega_0 - n v_m} - n v_m}{\omega_0 - n v_m} e^{v_m} - \frac{\omega_0 e^{\omega_0 + n v_m} + n v_m}{\omega_0 + n v_m}}$$

Where w_0 is the energy barrier inside the pore, n is the relative entrance length of the pore, and $v_m = qe, kT V_m$ is the non-dimensional transmembrane voltage. Assuming that the electric field inside the membrane is uniform, the transmembrane voltage is written as

$$V_m = E_* h$$

Where E_* is normal electric field?

The pore current density inside the membrane can be translated as an increase in the membrane conductivity using the relation

$$J_{cp} = \sigma_m E_*$$

The conductivity of the membrane at the points that pores are formed is calculated as

$$\sigma_m(t) = \sigma_{m0} + N(t) \sigma_p \pi r_p^2 K$$

Where σ_{m0} is the conductivity of the membrane before electroporation. The nonlinearity of the equation 3.4 comes from N which was described as

$$\frac{dN(t)}{dt} = \alpha e^{(V_m(t)/V_{ep})^2} \left(1 - \frac{N(t)}{N_0} e^{-q(V_m(t)/V_{ep})^2} \right)$$

Under equilibrium conditions maintain the transmembrane voltage below the required voltage of electroporation, which is about 1 V. Required voltage of nanoporation is the threshold at which notable increase in the density of the pores and membrane conductivity and consequently decrease in the transmembrane voltage occur. The increase in the transmembrane voltage leads to the increase of pore density which lowers the conductivity of the membrane and subsequently the transmembrane voltage.

B Design Consideration

The micro chip is designed in such a way that the pulsed electric field is absorbed and dissipated mainly in the biological medium placed between the electrodes within which cells to be treated are flowed. To do so, impedance matching is necessary between the generator, the transmission line and the nanoporation biochip considering the frequency spectrum of the applied pulses (typically 0–300 GHz); the electrical biochip behavior is mainly determined by the properties of the medium flowing within the micro fluidic channel. It can be explain by a parallel CG model, where C and G represent respectively the conductance and the capacitance of the biological medium .The electrically the capacitance and conductance are represented as $C = \epsilon_0 \epsilon_r \frac{hL}{d}$ and $G = \delta \frac{hL}{d}$ where ϵ_0 and ϵ_r represent respectively the conductivity and the relative permittivity of the biological solution, d corresponds to the gap between the electrodes containing the medium, h is the thickness of the micro channel and L the length of electrode in contact with the medium into the channel. The impedance Z of this model has to be matched to the impedance of psPEF generator in order to (a) deliver a maximum of energy to the biological medium, avoid reflections of the nsPEF backwards to the generator, avoid temporal distortions of the applied psPEF. The numerical equation of impedances is

$$Z = \frac{d}{A(\delta + j\epsilon_0 \epsilon_r \omega)}$$

Where $A = L \times h$ represent the area of the electrical current density. Considering the conductivity ($\sigma = 1$ S/m) and the relative permittivity ($\epsilon_r = 80$) of the used biological media, a transition frequency appears as $f = \frac{\delta}{2\pi \epsilon_0 \epsilon_r}$.and according to specified value $Z=100\Omega$ and frequency is near about 330GHz. In this thesis all these equation are followed to design the numerical model of proposed micro chip. Regarding that the impedance has to be matched for most of the spectrum of the applied FPGA based pico pulse exposure, to optimize the impedance and transition frequency for maximum utilization of pico electric field.

C. Electric field strength analysis

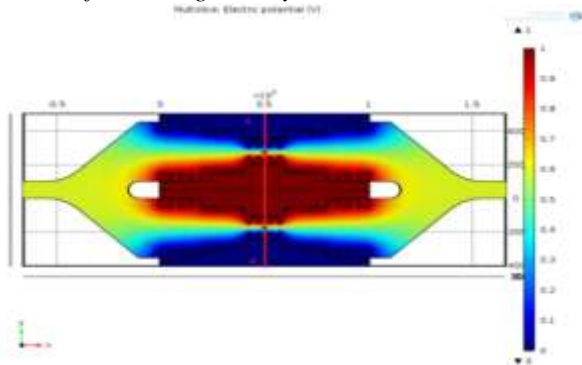


Fig 1: electrical field gradient within the 3D hybrid micro electrode.

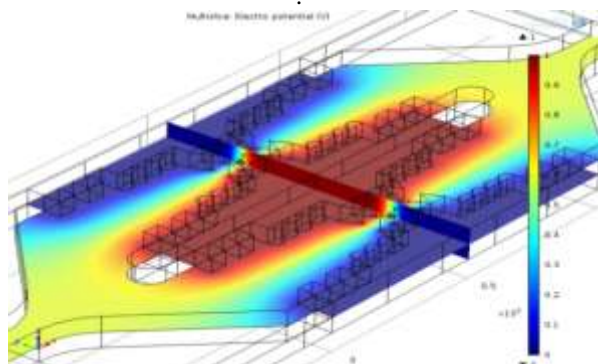


Fig 2 complete electrical potential distribution within the 3D hybrid micro chip.



Fig.3 Graphical view of electrical potential distribution with respect to height of the bi metallic electrode within the 3D hybrid micro chip.

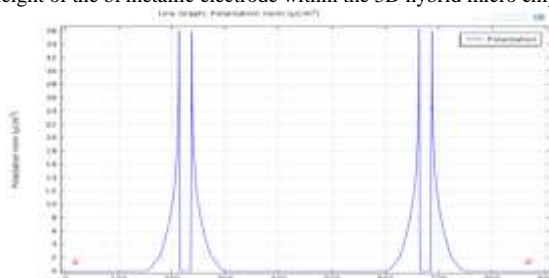


Fig.4 Graphical view of polarization with respect to height of the bi metallic electrode within the 3D hybrid micro chip

Fig 1 depicts the potential distribution with the proposed 3D micro chip where we find the non uniform distribution of potential and intra cellular organelle also effect by this field .At pole $\theta = 90^\circ$ And $\theta = 270^\circ$ the maximum potential are exposed which is similar as our numerical result. Fig.2 complete electrical potential distribution within the 3D hybrid micro chip. Where cell is

affected through the whole channel. Fig 3 shows the Graphical view of electrical potential distribution with respect to height of the bi metallic electrode within the 3D hybrid micro chip. It explore that the centre part (300-600) μm of the chip holds the maximum uniform potential where the nano pores are generated at the intra organelle. Fig. 4 shows the Graphical view of polarization with respect to height of the bi metallic electrode within the 3D hybrid micro chip which helps us to find out the maximum polarization area of Nono pores. Maximum velocity excreted at the centre of the chip, it affects the ion uptake of intra cellular unit of the rigid cell. All the information exposed in COMSOL simulation is as similar as numerical and experimental values of intra organelle nano poration of multi layer dense osteoblast cell.

D. Design layout

It is reported that the effective nanoporation in intraorganelle membrane or nucleolus membrane need specific type of pulse, micro chip and suspension media. The author explores in the section 3.5.1. that the optimum value of the applied pulse having the duration of 5 pico second , pulse intensity of 1 volts is suitable and effective intraorganelle nanoporation of osteoblast cell. it also exposed that intraorganelle nanoporation can easily obtained if the shape of the electrode is triangular or saw tooth which are made by gold bismuth alloy in specified micro channel having the height and width of micro -fluidic channel should be moderate and same & it would be taken as 200 micrometer for successful and effective intraorganelle nanoporation. The resistances of micro channel should be as high as possible for above purpose. With the help of above discussion the author optimised the system and designs a simulating micro fluidic chip on the bases of following specification with in which the osteoblast cell is placed, to explore the numerical and analytical characterization of intraorganelle nanoporation. The simulation tool is composed of a $100\mu\text{m}$ thick SU8 micro fluidic channel including thick bi metallic electrode (Bi and Au) electrodes with a typical thickness of $50\mu\text{m}$, in which cells suspended in a biological medium are injected. Bi-metallic is chosen as material for the electrodes because of its excellent electrical properties and bio compatibility. The biochip is designed in such a way that the pulsed electric field is absorbed and dissipated mainly in the biological medium placed between the electrodes within which cells to be treated are flowed.

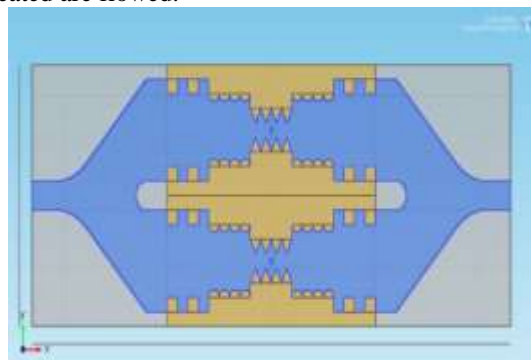


Fig 5 Dimension and design of microelectrode and micro channel within the 3D hybrid micro chip (Top view).

Figure 5 shows the top view of nanoporative devices. This numerical model satisfy the all simulating and analytical values of intra organelle nanoporation. Length, Height & Width of the microchip are 2300 , 100, 900 μm respectively. The inlet and outlet path are same i.e 10 μm . Within the micro chip a non uniform sidewall having the mixed dimension micro-electrode is places which is made by bismuth and gold. The shape of this electrode is the combination of three different shaped electrodes. The central part consists of triangular, medial part consists semicircle and terminal part attached with square shaped electrode. The length, width and height of the micro electrode are 1000,900,100 μm .as the electrode is hybrid in nature so inter electrode gap is non uniform throughout the whole micro channel. The inter electrode distances of central, medial and lateral part are 50,150,250 μm respectively. The dimension of micro electrode so the remaining part i.e. the micro channel is specified by Length, Width, Height and their dimension are 2300,250,100 μm . It shows the complete structure of the intrigrated devices.

E Micro fabrication of nanoporative devices.

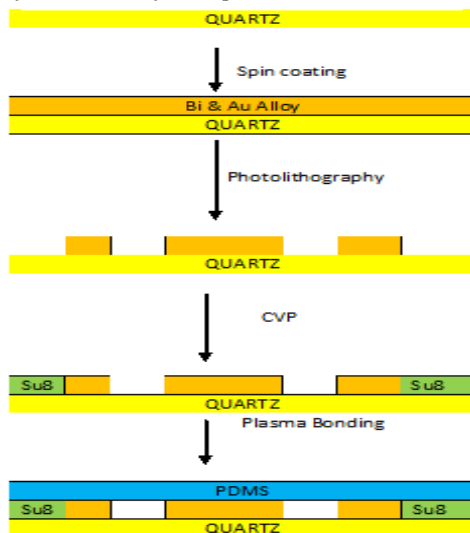


Fig 6: Fabrication steps of 3D micro chip

To make the pattern of electrodes we use the glass substrate. The glass substrate was pre-cleaned with RCA-1 solution (mixture of de ionized (DI) water, ammonium hydroxide (NH4OH) and hydrogen peroxide (H2O2) in a 5:1:1 ratio), followed by rinsing three times in DI water and is used as the main support for transparent and planar surfaces at the end of the process. From this seed layer, electroplating of 50 μm Bismuth and gold electrodes is achieved using an electrolytic bath based on potassium aurocyanure (KAu (CN) 2). Then a standard UV photolithography using a commercial photo resist is used to define the electrode shapes. Removal of the excess Bismuth and gold alloy is made on the different parts of the device by wet etching with a solution based on potassium iodide. Then the Cr seed layer is chemically etched. After the removal of the photoresist and the cleaning of the wafer by successive baths of acetone, ethanol and water combined with ultrasonic steps, the micro fluidic channels are defined by a UV photolithography of a transparent commercial

photoresist, which allows reaching a high aspect ratio (SU8-2025, Micro Chem). The SU8 layer is 25 μm thick to reach the total thickness of the micro fluidic channel set to 50 μm . To finish, the biochip is packaged using a PDMS membrane. This layer is bonded to the SU8 resist using a silanization process based on (3-aminopropyl) trimethoxysilane (Aldrich) and methanol mixture. The febrication process is shown in figure 6.

V. EXPERIMENTS

A Set up for intrigrated intraorganelle nanoporation system

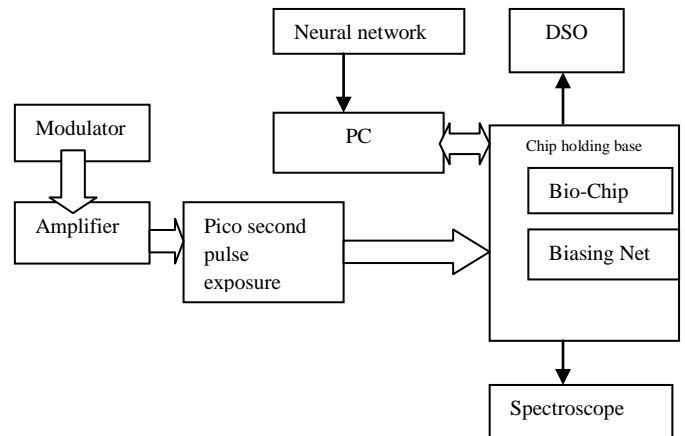


Fig.7: Block diagram of intrigrated intraorganelle nanoporation system:

Figure 7 reflects the block diagram of intrigrated intraorganelle nanoporation system which consist of bio chip holding base ,pico pulse exposure, neural network, spectroscope and personal computer (PC).The bio chip holding unit used for properly places the micro chip along with input and output syringe pump. The high intense programmable pico pulse exposure provides dedicated suitable pulse to the micro chip. Neural network is used for efficient intra organelle nanoporative image reorganization and output image is exposed through spectroscope and digital storage oscilloscope. The complete set up is control by PC.

B Effect of Pico pulse for intraorganelle nanoporation:

As it is reveals that the pico pulse signal has an important role for nanopore formation within the intraorganelle or nucleolus membrane so author gives an extra concentration for the design of pico pulse generator. To obtain the perfect pico signal the author smart control FPGA technology and the following schematic diagram is used for simulation of pico pulse ,which is applied to the COMSOL simulated 3D hybrid micro chip ,that provide the best option for intraorganelle nanoporation of rigid osteoblast cell. The simulating pico pulse electric field expose system is describe bellow

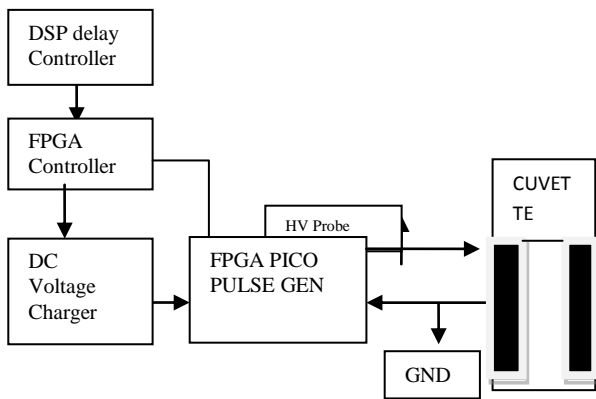


Fig.8: Pico second pulse electric field exposure

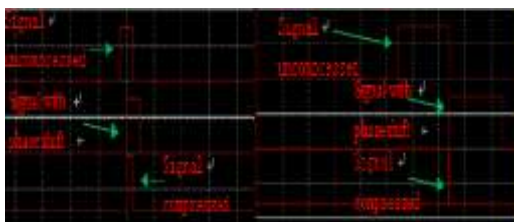


Fig: 9 simulated graph for FPGA control pico pulse generator.

The figure. 8, and 9 shows the pico pulse electric field exposure system. The exposure set-up is composed of Pico second pulse generator unit, high voltage probe, DSP delay controller, FPGA controller, and FPGA based pico pulse generator which allow delivering the pulses to the biological medium. Pico pulse is generated by embedded FPGA programmable pulse generator which is shown in figure 1 and it is monitored by FPGA controller and. The pulsing sequence was controlled by a DSP delay controller. The voltage waveform was monitored using a voltage probe. The voltage in the final pulse was slightly reduced due to medium temperature rise. The medium temperature during pulsing was monitored using a fast radiation thermometer (RT) with a response time of 10 ms, sufficiently fast to monitor the overall temperature change during the repetitive pulsing. The applied voltage across the biochip electrodes is measured by a HV probe .The probe has a large frequency bandwidth (6 GHz) and is designed to have the output terminated into the system with a voltage ratio of 1:10. For the measurements, the two conductor pins of the probe are placed in direct contact with the input or output of the gold bismuth electrodes.

5.2 Experimental Process:

In this study the experimental biological tests are performed with 20 ps duration pulses. A train of 200 psPEF, square shaped, 20 ps duration is applied with a repetition frequency of 234 Hz. A view (fluorescence or bright field microscopy) of cells within the 3D hybrid micro chip is recorded before and just after the application of psPEF. As shown in fig. 14, Cells fluoresce in red after the application of psPEF, proving that PI introduces into the cytosol, due to the disturbance of the plasma membrane, Note that the observation is made with functional cells located in the

white circles drawn on this figure .Viability of cells submitted to psPEF treatment was checked thanks to Trypan Blue test. An average of $90 \pm 1\%$ of exposed cells remains still alive 30 min after being exposed to ps PEF. The number of nano pulses that were applied (200 or 300 pulses), to confirm the effect of these parameters on the intra cellular nanoporation .As expected, the number of pulses and their amplitude both influence the level of permeabilization. These preliminary characterizations of the effect of nanoporation on intra organelle, in particular on the permeabilization of the plasma membrane, were permitted thanks to the real time Observation on the miniaturized bio device. Deeper exploitation of this type of device will be conducted together with the development of new psPEF generators. Actual results demonstrate the capability of the developed 3D hybrid bio micro chip to address the effect of psPEF to the intra organelle nanoporation of multilayer osteoblast cell within the micro chip.

Table: IV Percentage of permeabilized cells depending both on the number and amplitude of applied psPEF.

C Experimental Data:

Table IV: Percentage of permeabilized cells

Condition	No of pulse	% of permeabilizations
Applied electric field (KV/Cm)		
30	150	58
35	175	60
40	200	72
45	200	85
45	250	87
50	250	90
50	300	95

The above table shows the percentage of permeabilized cells depending both on the number and amplitude of applied electric field. By the influences of above pulse it is observed that at pico pulse a large amount of dedicated chemicals entered into the intra organelle and all experimental values are explored through the graph shown in figure 9.

Table: V: Variation of flu recent intensity with pulse duration.

Pulse duration (X-axis) second	Flu recent intensity (Y-axis)no of molecules
10^{-6}	0
10^{-7}	10,000
10^{-8}	15,000
10^{-9}	20,000
10^{-10}	40,000
10^{-11}	80,000
10^{-12}	100,000
10^{-13}	100,000
10^{-14}	100,000

The above experimental values are represented by the graph bellow.

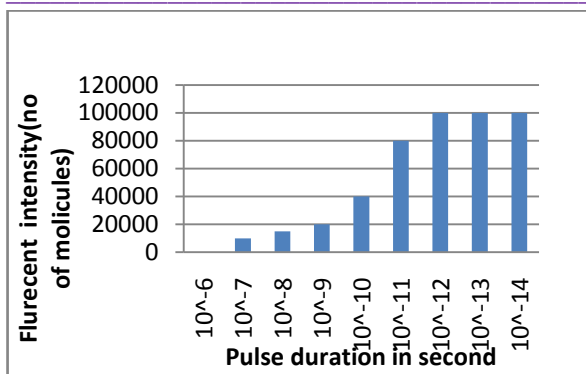


Fig 10: Microscopic real-time image of a typical osteoblast cell undergoing PI uptake.

The effects of picosecond electrical pulses on the intra organelle are also demonstrated by the uptake of dyes and the orientation of phosphatidylserine in the membrane after applying pulses. Three of the dyes most often used to study changes in plasma membrane permeability are trypan blue, propidium iodide (PI), and ethidium homodimer. The above figure 10 shows the uptake of PI by osteoblast cells. It is interesting that the increase in fluorescence is observed only after approximately 12 minutes and then completed in one minute. This indicates that the formation of pores large enough to allow passage of propidium iodide is a secondary effect, following the formation of nanopores, which occurs on a picosecond timescale. It is likely that the nanopores are too small to allow PI uptake immediately and the secondary PI uptake is due to rapture of intra organelle.

Table Variation of mean and STD error with pulse duration.

Pulse duration	Electric field	% of Osteoblast cell		
		Mean	Std error	≥ 15 unit increase in gray scale intensity After application of electric field.
100 ns	30 KV/cm	10	5	
	60 KV/cm	32	10	
10ns	30 KV/cm	7	5	
	60 KV/cm	15	10	
100ps	30 KV/cm	22	7	
	60 KV/cm	68	10	
10ps	30 KV/cm	16	7	
	60 KV/cm	38	10	

The measurements performed with pulses of various durations, ranging from 10 ns to 100pns, showed a clear tendency: the effects of relatively long (nanosecond) pulses on membrane integrity occurred rapidly, suggesting a direct effect upon the intraorganelle nanoporation. In contrast, the effects of shorter pulses were delayed, suggesting a secondary/indirect effect on the intraorganelle. The application of long pulses (100 ms) in the first minute of an experiment resulted in PI uptake in the above table. In all

except the 10ps pulse conditions, increasing pulse amplitudes were associated with increasing percentages of cells taking up PI. The spatial development of dye uptake was also examined for nanosecond and picoseconds pulses. For long pulses, onset of fluorescence uptake followed shortly after pulse application, and fluorescence increased more rapidly in that part of the nucleus oriented toward the anode. For shorter pulses, onset of fluorescence was delayed and the spatial development of the fluorescence occurred without obvious orientation to the direction of the applied electric field. Thus, for long pulses, surface membrane integrity was lost immediately with anodic preference; for short pulses, loss of surface membrane integrity was delayed and did not have a discernable electrode preference. The changes in cell morphology induced by long pulses were most striking: cells went from showing somewhat retractile edges with little intracellular detail visible before pulse application, to diminished retractile edges and appearance of intracellular detail.

D Observation

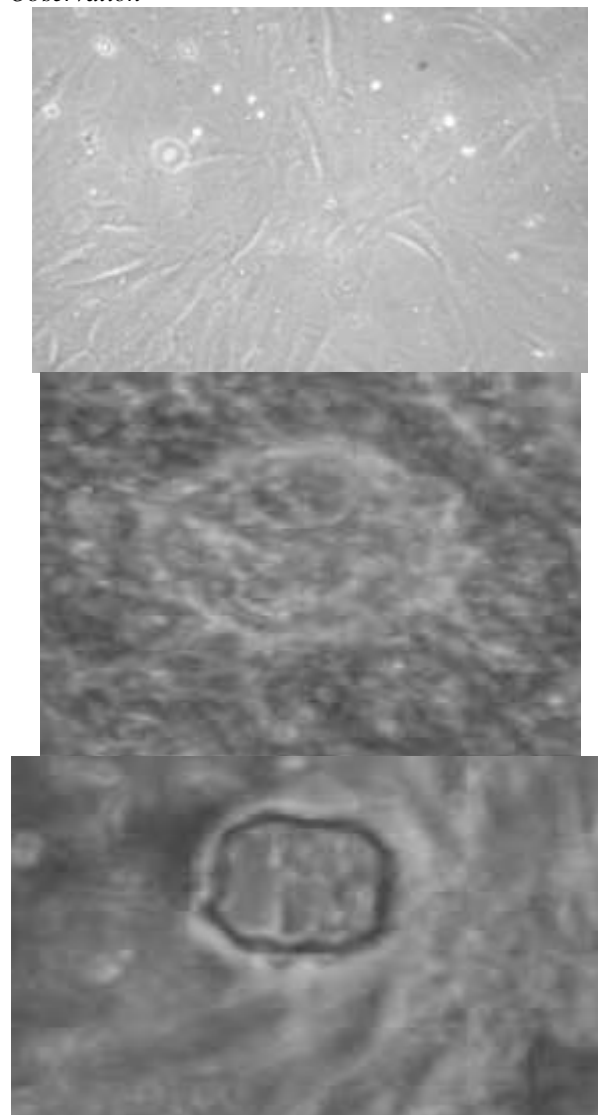


Fig11: Morphological views of intra organelle Nano Poration of osteoblast cell in 3D hybrid micro chip. (a) Dense osteoblast cell, (b) before intra organelle nano poration(c) after intra organelle pico poration.

Figure 11 shows the morphological changes of osteoblast cell. In fig 11(a) dense osteo cell. When the micro pulse is applied the cell starts to response but it is unable to penetrate the cell membrane which is exposed in fig 11(b), expected results will come when we apply the Pico pulse on the cell, a number of nano pores are generated on the intra organelle and chemicals are entered into the cell, that shows in the figure 11(C).From this observation it is exposed that there is no effect of micro pulse but pico pulse penetrate the on intraorganelle .It supports the numerical and analytical result explore in this research.

VI. INTRAORGANELLE NANOPORATION:

The experimental results are plotted and following graphs are obtained

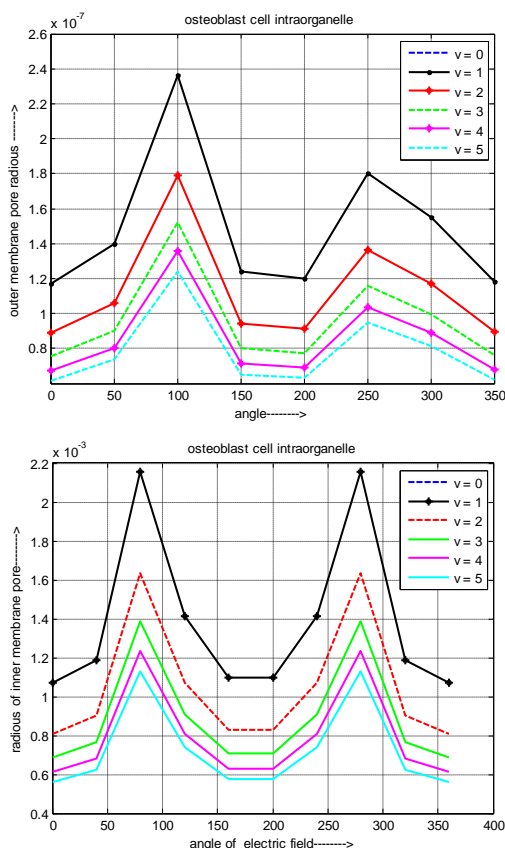


Fig 12: Evaluation of the intra organelle pore radius (a) outer membrane (b) inner membrane

The figure 12 explores the variation of intra organelle pore radius along with pole position of applied electric field for intraorganelle outer membrane (a) and innermembrane (b). It clears that the radius of all the pores are not same it is sinusoidal distributed over the outer and innermembrane. The radius of pore at outer membrane is lower than innermembrane and location of biggest nanopores are different for both layers. As the nanopores are created, intra organelle potential increases and the biggest nanopores move just opposite to the equator (E). It is also shown that pore radius is gradually increase as the angle of applied electric field is increase & maximum pore radius is obtain at an angle of $\theta = 90$ and $\theta = 270$ for inner membrane and $\theta = 100$ for outer membrane which is independent of pulse, electrode, micro channel and

suspension media specification. After that it starts decrease but for both layers the radius of the nanopores inversely proportional with the amplitude of applied electric pulse. The author also fined out that the pore radius of outer membrane is greater than the radius of inner membrane of the organelle due to the higher elasticity of layers. It reflects the different molecular structure of inner part of the organelle.

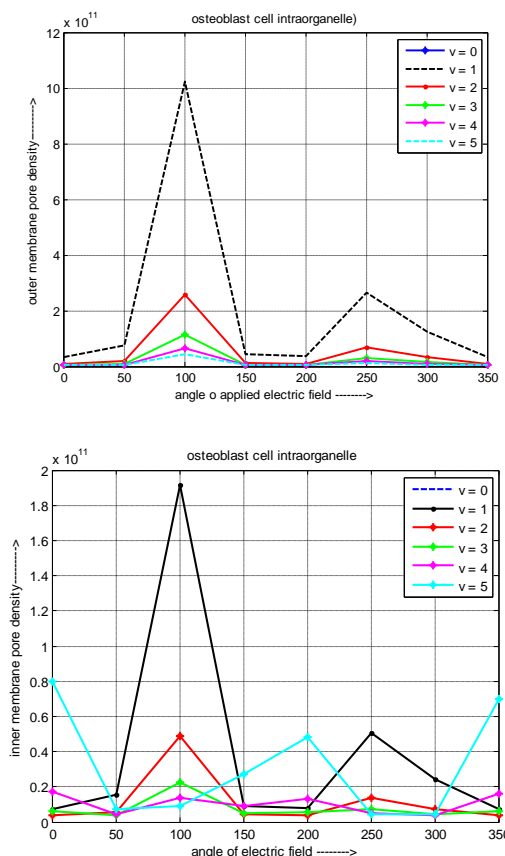


Fig 13: Evaluation of the intra organelle pore density (a) outer membrane (b) inner membrane

The figure 13 depicts the variation of intra organelle pore density along with pole position of applied electric field for intraorganelle outer membrane (a) and innermembrane(b).In case of pore density the pulse specifications have an acceptable effect although the maximum pore density locate at the pole ($\theta = 100$ & 250) for both layers which is independent of above variations. The effectiveness of pulse specification on inner membrane pore density is same as outer membrane but the value of pore density of inner membrane is low compare to outer membrane of the organelle. This information reflects that the outer membrane is more permeable than inner membrane but maximum pore density lies in the same pole ($\theta = 100$ & 250) for both layers. Author also fined that in inner membrane pore density is inversely related to the amplitude of pulse. For drug delivery system it is needed the maximum pore density region which is exposed through this graphical analysis.

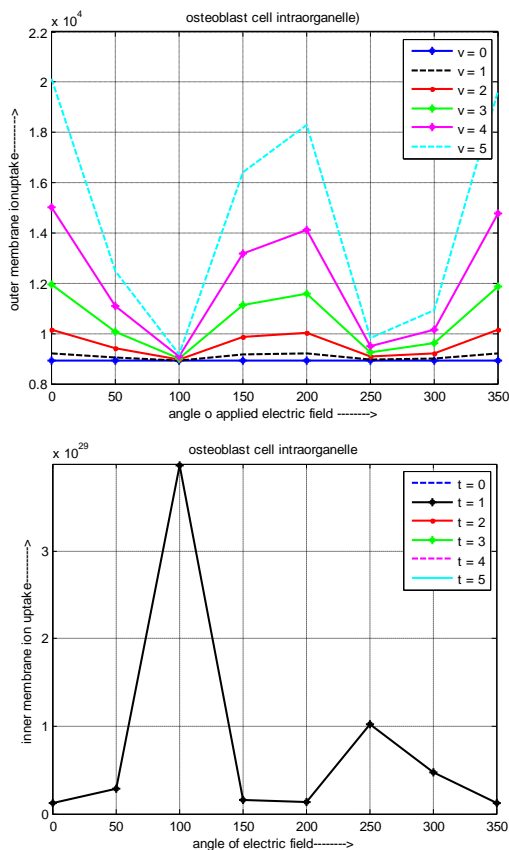


Fig 14: Evaluation of the intra organelle ion uptake (a) outer membrane (b) inner membrane

The figure 14 shows the variation of intra organelle ion uptake along with pole position of applied electric field for intraorganelle outer membrane (a) and innermembrane (b). It is explored that the amount of ion which is uptake by the intra organelle is only occurred at pico scale pulse and its value is not same throughout the whole surface of the layer of the nucleus. It is changed sinusoidal in nature over the surface. The maximum ion uptake occurs at pole $\theta=0$ & 360 and zero value exposed at pole ($\theta=100$ & 250) where the surface tension is minimum and it implies that such part of membrane will inherently have an inverse Kelvin vapor pressure effect, that resulting in increased water condensation. The effectiveness of pulse, electrode, micro channel and suspension media on inner membrane ion uptake is same as outer membrane but the value of intra organelle is low compare to outer membrane. This information reflects that the outer membrane is more permeable than intra organelle.

VII. CONCLUSION

The current research explores the new Novel 3D hybrid micro bio device optimized for the psPEF exposure of intra organelle nanoporation. In this paper the effect of the automatic controlled FPGA based pico second pulse on intra cellular organelle nano poration is addressed. The effect of important parameters specially intra cellular pore density, ion uptake and developed pressure on intra organelle is studied and explore the understanding of biological mechanisms, which can occur during

nanoporation of multi layer dense osteoblast cell. It is observed that When the micro pulse is applied the cell starts to response but it is unable to penetrate the cell membrane where as the expected results will come when we apply the Pico pulse on the cell, a number of Nano pores are generated on the intra organelle and chemicals are entered into the cell. On the other hand we also find out that ,in case of pore density the pulse specifications have an acceptable effect although the maximum pore density locate at the pole ($\theta = 100$ & 250) which is independent of specification of pulse and micro chip. As we know the pore density of the organelle has great influences on ion uptake and in our study it is explored that the amount of ion which is uptake by the intra organelle is only occurred at Pico scale pulse and its value is not same throughout the whole surface of the layer of the nucleus. It is changed sinusoidal in nature over the surface. The maximum ion uptake occur at pole $\theta = 0$ & 360 and zero value exposed at pole ($\theta = 100$ & 250) where the surface tension is minimum. As a whole the complete nanoporation of intra organelle is characterized in this research paper.

We also report the numerical and analytical model of intra organelle nano poration of multi layer osteoblast cell placed in a 3D hybrid micro biochip under the influences of FPGA based ultra sonic pico second pulse generator. The reported study encourage the specific micro chip multiple dimension micro channel with irregular bi metallic (Bi and Au) side wall electrodes that are designed to deliver a maximum of energy to the biological medium containing multilayer osteoblast cell. Finally this numerical model also supports the faithful pattern reorganization of biological cell image after intra organelle nanoporation using neural fuzzy network which is first time implement for nanoporation. The reported nanoporative device aided by a quantitative understanding of the interactions between cells and an external electric field. The micro device is effective in more advantageous conditions than conventional systems, small voltages and power consumptions, continuous flow, small sample volume, and negligible heating.

In summary, the present data provide evidence that psPEF introduce the ions with specified microchip possibly through the nucleus mediated pathway. The use of picoseconds pulses not only allows us to enter a new field of field-cell interactions, but it may open the door to a range of noninvasive therapeutic applications. This research also explores the non-uniform natures of nanopores and electro mechanical property of outer and inner layer of intraorganelle .Further studies are needed to elucidate the osteoblast cell responses to psPEF in detail within the micro fluidic environment at radio frequency.

REFERENCES:

- [1] A.G. Pakhomov, D. Miklavcic, M.S. Markov (Eds.) Advanced Electroporation Techniques in Biology in Medicine, CRC Press, Boca Raton, p. 528(2010).
- [2] A.G. Pakhomov, J.F. Kolb, J.A. White, R.P. Joshi, S. Xiao, K.H. Schoenbach, Long-lasting plasma membrane permeabilization in mammalian cells by nanosecond

- pulsed electric field (nsPEF), *Bioelectromagnetics* 28 655–663(2007).
- [3] B. L. Ibey, A. G. Pakhomov, B. W. Gregory, V. A. Khorokhorina, C. C. Roth, M. A. Rassokhin, J. A. Bernhard, G. J. Wilmink, and O. N. Pakhomova, “Selective cytotoxicity of intense nanosecond duration electric pulses in mammalian cells,” *Biochim. Biophys. Acta*, vol. 1800, no. 11, pp. 1210–1219, (2010).
- [4] Buescher, E.S., Smith, R.R., Schoenbach, K.H., Submicrosecond intense pulsed electric field effects on intracellular free calcium: mechanisms and effects. *Plasma Science, IEEE Transactions on* 32(4), 1563-1572(2004).
- [5] E. Neumann, A.E. Sowers, C.A. Jordan (Eds.), *Electroporation and Electrofusion in Cell Biology*, in, Plenum, New York, (1989).
- [6] G.L. Andreason, *Electroporation as a technique for the transfer of macromolecules into mammalian cell lines*, *J. Tiss. Cult. Meth.* 15. 56-62(1993).
- [7] G. Saulis and M. S. Venslauskas, “Cell electroporation. Part 2. Experimental measurements of the kinetics of pore formation in human
- [8] G. Saulis, and R. Saul’ė, “Size of the pores created by an electric pulse: Microsecond vs millisecond pulses,” *Biochim. Biophys. Acta, Biomembrances*, vol. 1818, no. 12, pp. 3032–3039, (2012).
- [9] Hartig, M., U. Joos and H-P Wiesmann.. *Capacitively coupled electric fields accelerate proliferation of osteoblasts-like primary cells and increase bone extracellular matrix formation in vitro.* *Eur Biophys J* 29:499-506(2000).
- [10] K.H. Schoenbach, S.J. Beebe, E.S. Buescher, *Intracellular effect of ultrashort electrical pulses*, *Bioelectromagnetics* 22 ,440–448(2001).
- [11] K.H. Schoenbach, *Bioelectric effect of intense nanosecond pulses*, in: A.G. Pakhomov, D. Miklavcic, M.S. Markov (Eds.), *Advanced Electroporation Techniques in Biology in Medicine*, CRC Press, Boca Raton, , pp. 19–50(2010).
- [12] Marszalek, P., D. S. Liu, and T. Y. Tsong.. *Schwan equation and transmembrane potential induced by alternating electric field.* *Biophys.J.* 58:1053–1058(1990).
- [13] Morse, P. M., and H. Feshbach.. *Methods of Theoretical Physics.* McGraw-Hill, New York, NY(1953).
- [14] P.T. Vernier, Y. Sun, M.A. Gundersen, *Nanoelectropulse-driven membrane perturbation and small molecule permeabilization*, *BMC Cell Biol.* 7 - 37(2006).
- [15] Sreedharan V, Zhang D.. *Finite element modelling of cellular responses of gap junction connected osteocytes under extremely low-frequency electromagnetic fields.* *Bioengineering, Proceedings of the Northeast Conference:*160-161(2003).
- [16] T. Kotnik, D. Miklavcic, *Theoretical evaluation of voltage inducement on internal membranes of biological cells exposed to electric fields*, *Biophys. J.* 90 ,480–491(2006).
- [17] Tsong, T.Y., *Electroporation of cell-membranes.* *Biophysical Journal* 60(2), 297-306(1991).
- [18] Vernier, P.T., Sun, Y.H., Gundersen, M.A., *Nanoelectropulse-driven membrane perturbation and small molecule permeabilization.* *Bmc Cell Biology* 7(2006).
- [19] W. Frey, J.A. White, R.O. Price, P.F. Blackmore, R.P. Joshi, R. Nuccitelli, S.J. Beebe, K.H. Schoenbach, J.F. Kolb, *Plasma membrane voltage changes during nanosecond pulsed electric field exposure*, *Biophys. J.* 90 3608–3615(2006).